

Supporting Information

Lanthanide-supported molybdenum–vanadium oxide clusters: syntheses, structures and catalytic properties

Fei Fei, Haiyan An,* Changgong Meng, Lin Wang, Huilong Wang

College of Chemistry, Dalian University of Technology, Dalian 116023, P. R. China

CONTENTS:

I. Supplementary Structure Figures

II. Supplementary Physical Characterizations

III. Supplementary Catalysis Section

IV. Supplementary Tables

V. Supplementary Schemes

I. Supplementary Structure Figures

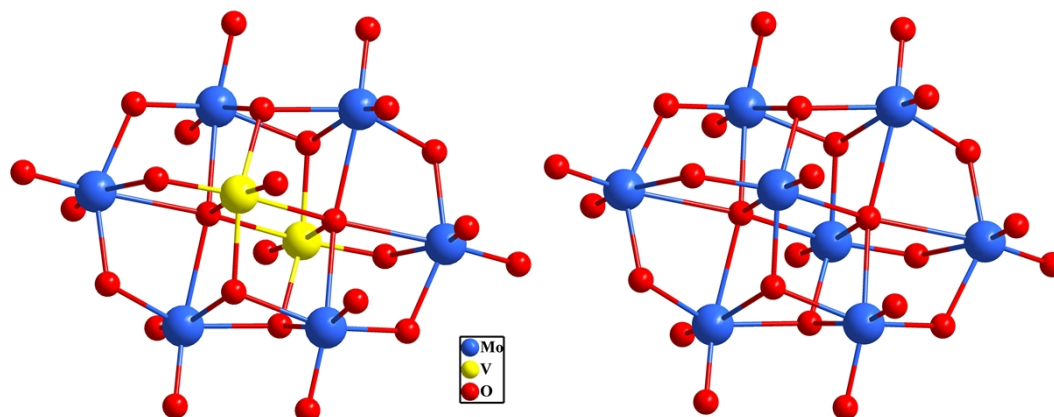


Fig. S1 Ball-stick representation of β -[Mo₆V₂O₂₆]⁶⁻ anion in **1** and the β -[Mo₈O₂₆]⁴⁻ anion.

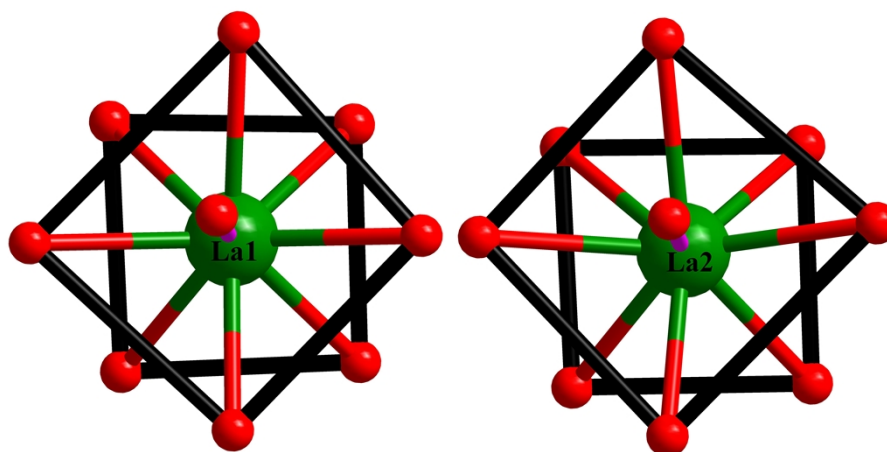


Fig. S2 Ball-stick representation of the monocapped square antiprismatic coordination modes of La(1) and La(2) cations in **1**.

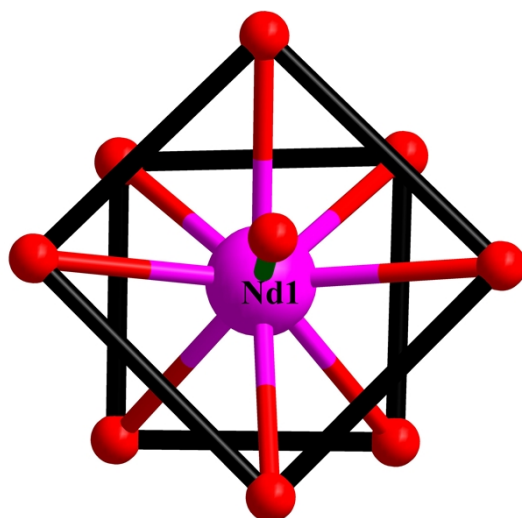


Fig. S3 Ball-stick representation of the monocapped square antiprismatic coordination modes of Nd(1) cation in **3**.

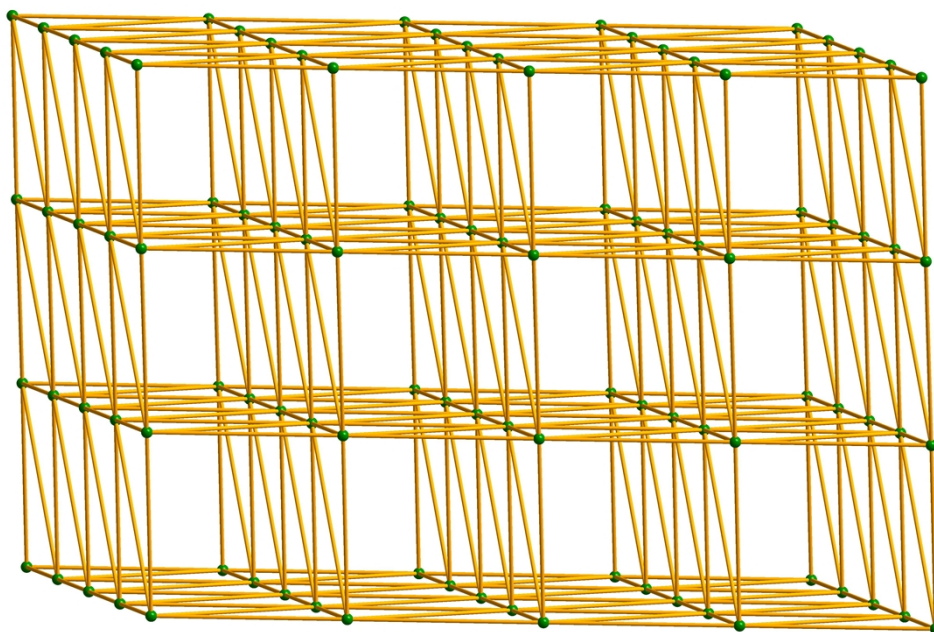


Fig. S4 Schematic representation of the 8-connected topology of **1**.

II. Supplementary Physical Characterizations

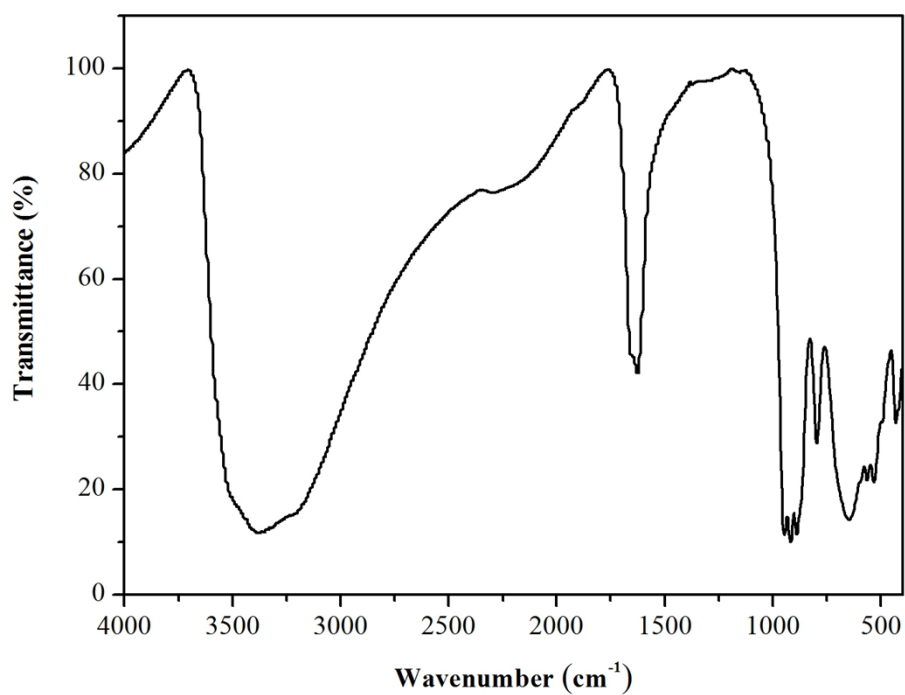


Fig. S5a IR spectrum for compound 1.

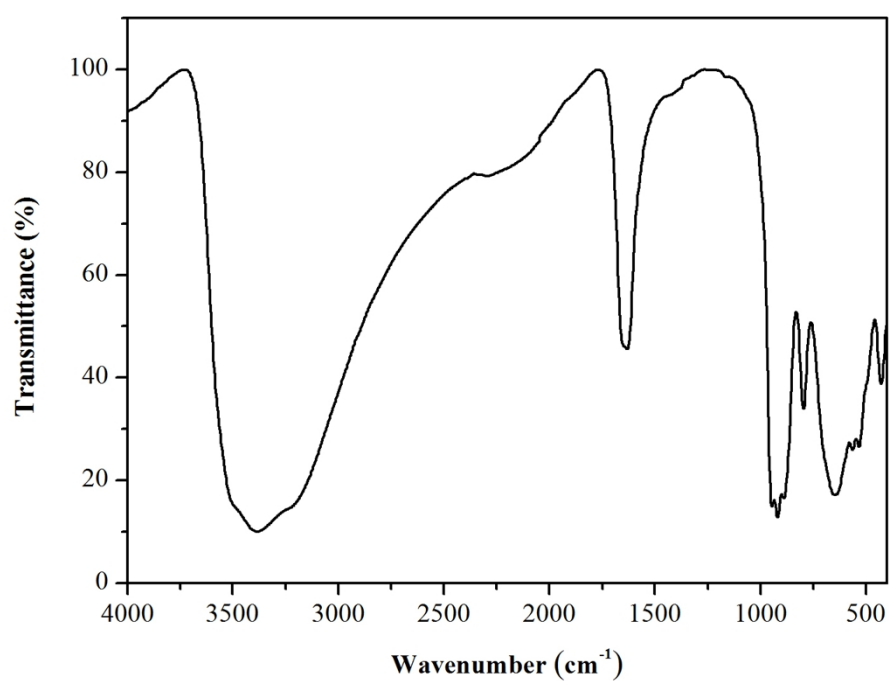


Fig. S5b IR spectrum for compound 2.

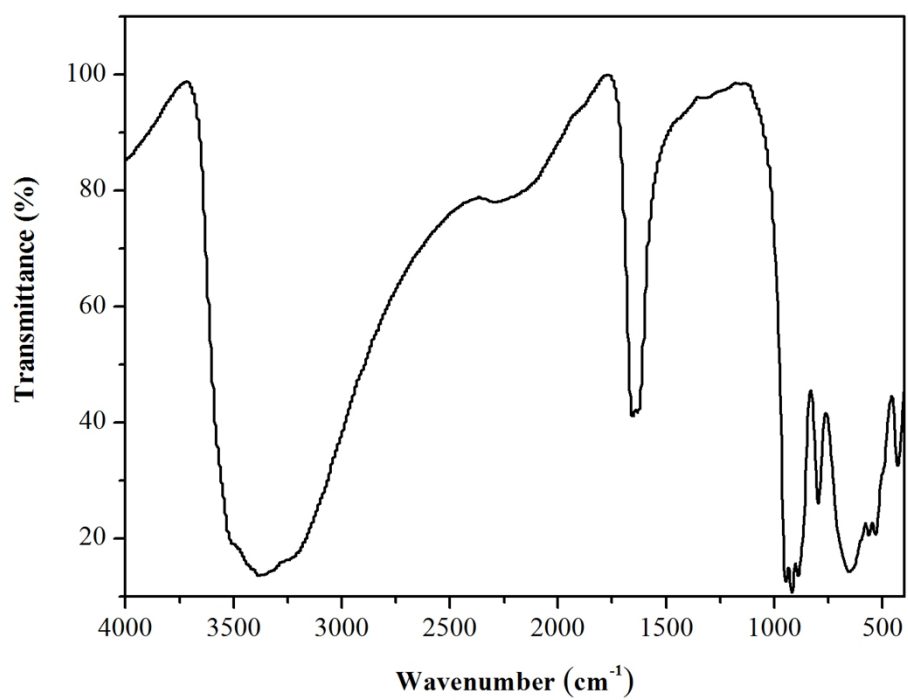


Fig. S5c IR spectrum for compound **3**.

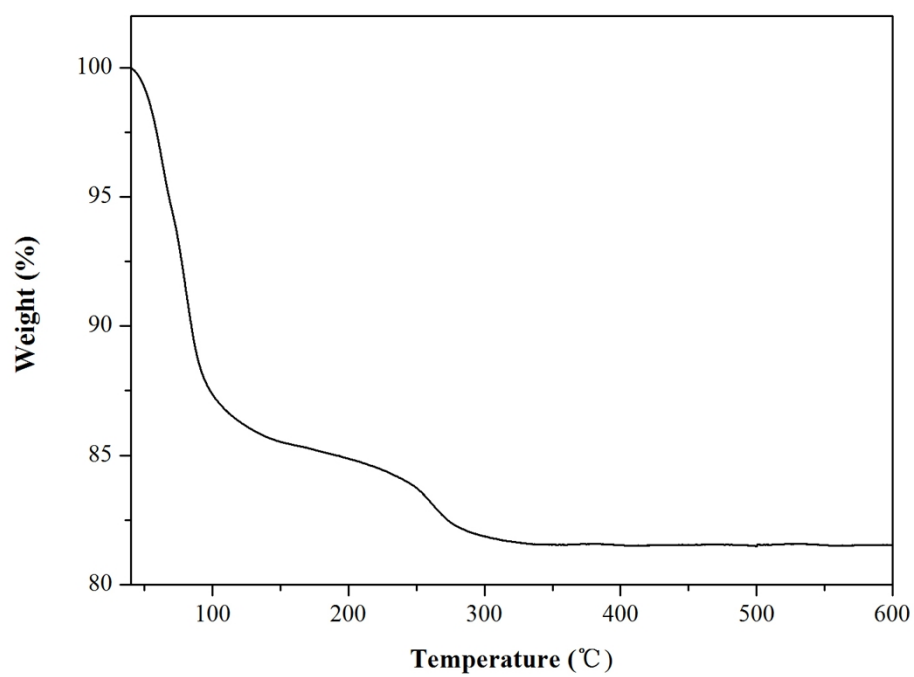


Fig. S6a TG curve for compound **1**.

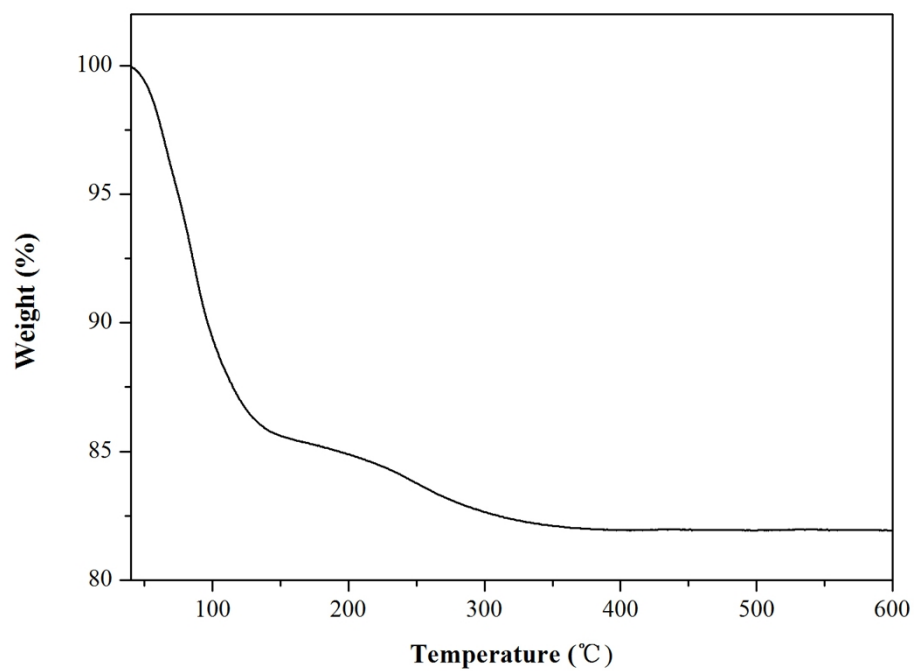


Fig. S6b TG curve for compound 2.

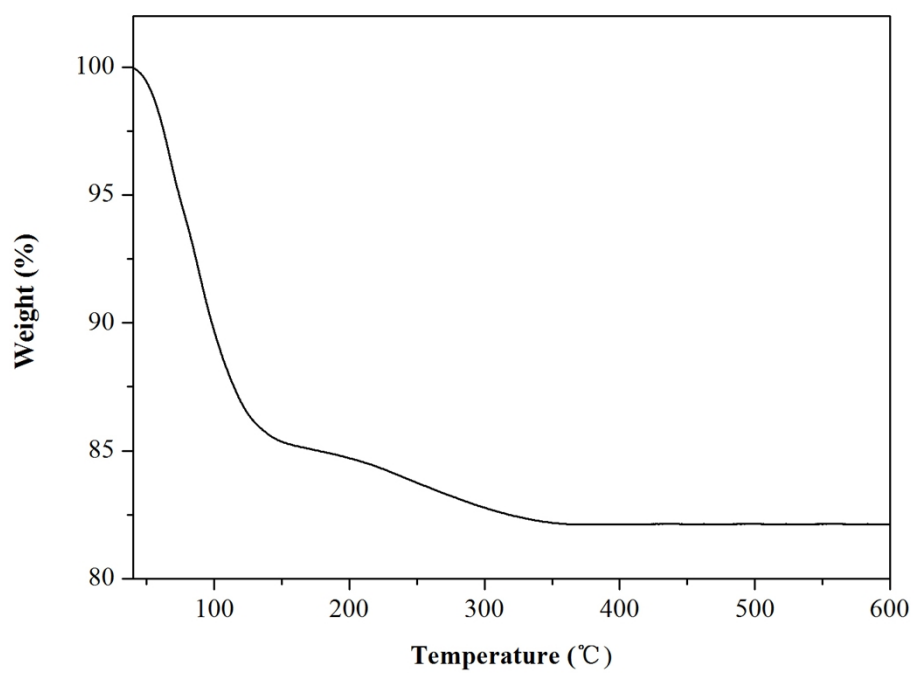


Fig. S6c TG curve for compound 3.

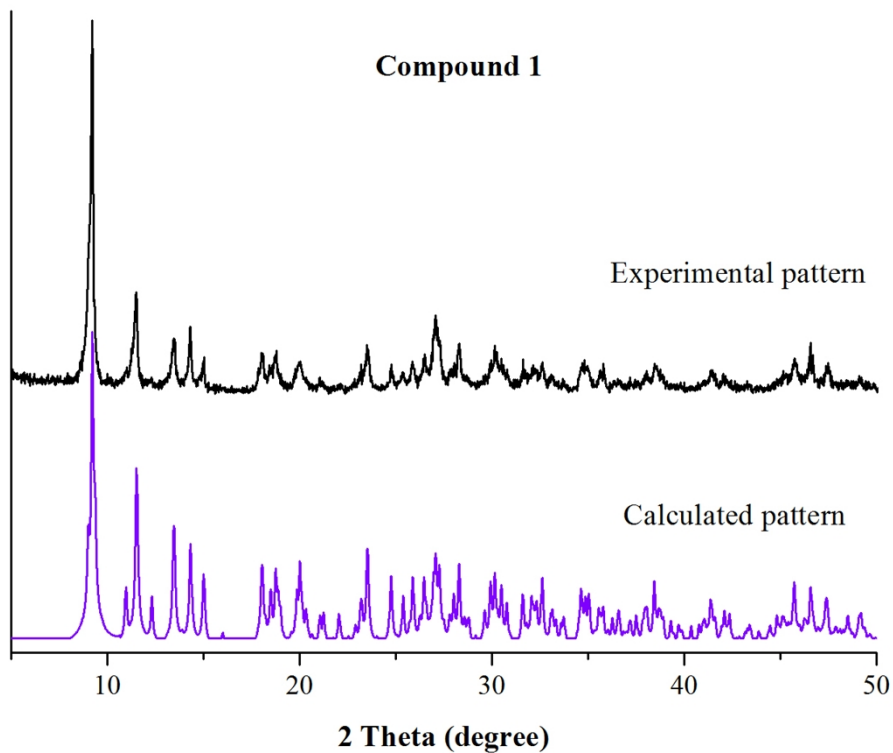


Fig. S7a The calculated and experimental PXRD patterns for compound 1.

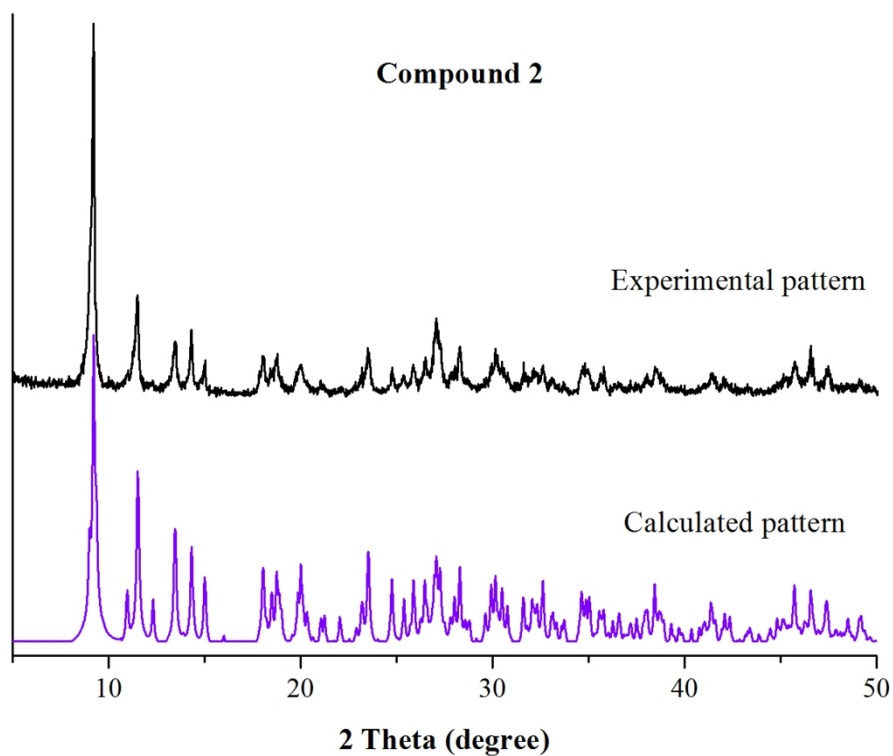


Fig. S7b The calculated and experimental PXRD patterns for compound 2.

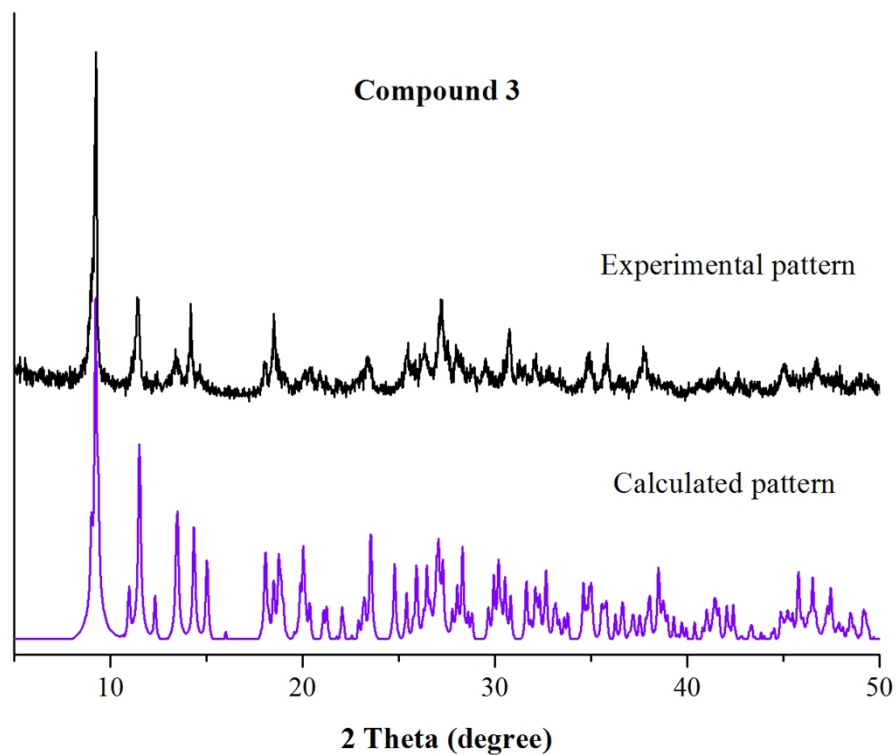


Fig. S7c The calculated and experimental PXRD patterns for compound **3**.

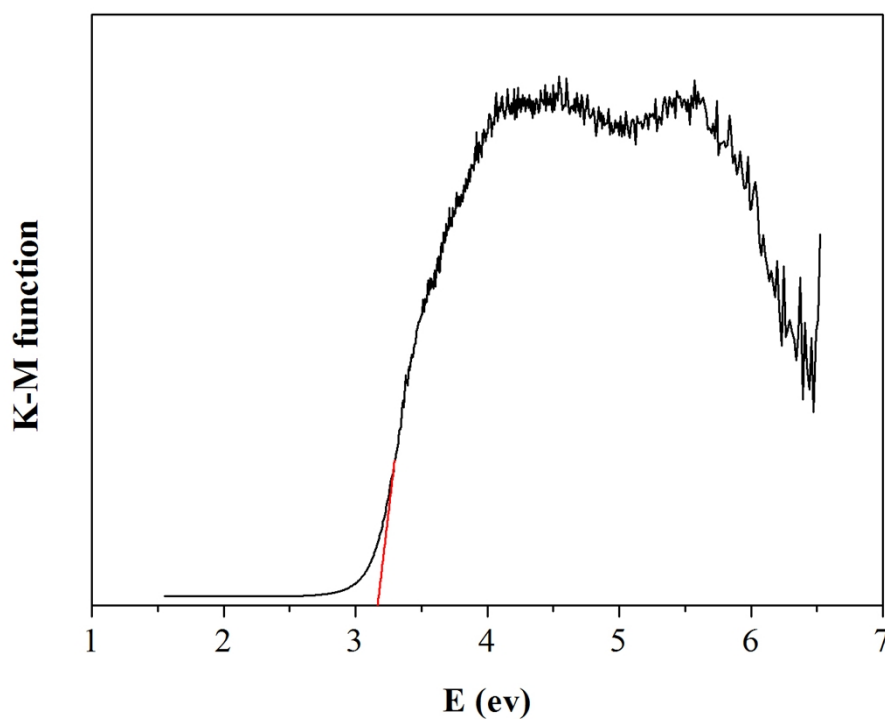


Fig. S8 UV-vis-NIR diffuse reflectance spectra of K-M functions vs energy (eV) of the precursor $K_5NaMo_6V_2O_{26} \cdot 4H_2O$.

III. Supplementary Catalysis Section

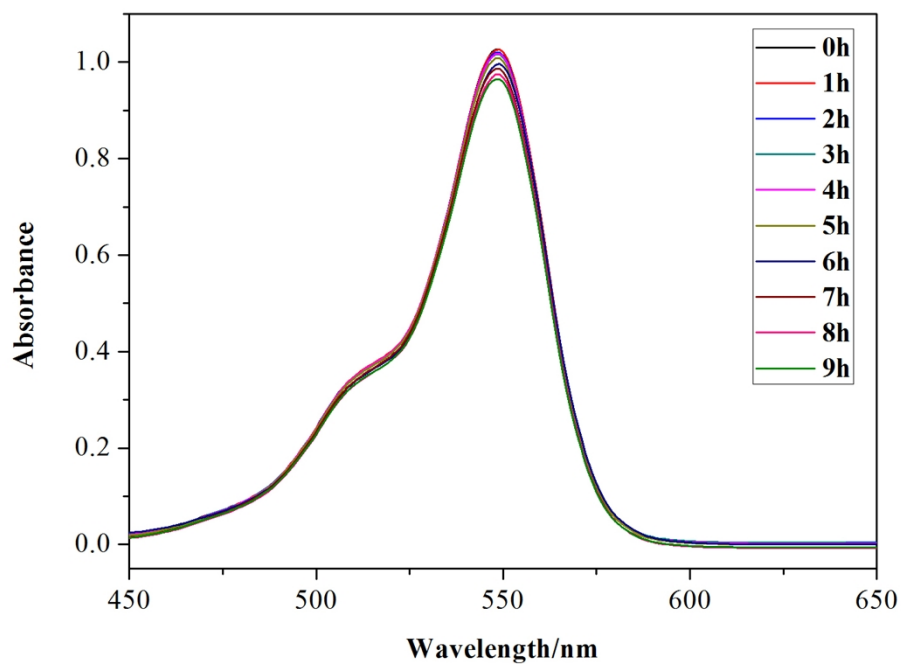


Fig. S9 UV-Vis absorption spectra of RhB solution during the decomposition reaction without catalyst.

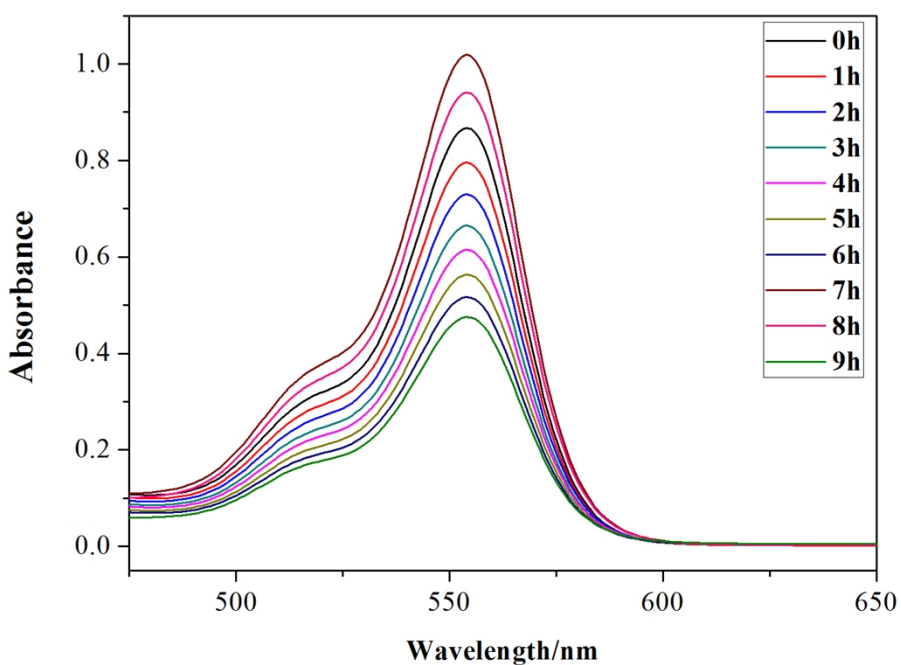


Fig. S10 UV-Vis absorption spectra of RhB solution during the decomposition reaction with the use of $K_5NaMo_6V_2O_{26} \cdot 4H_2O$ as catalyst.

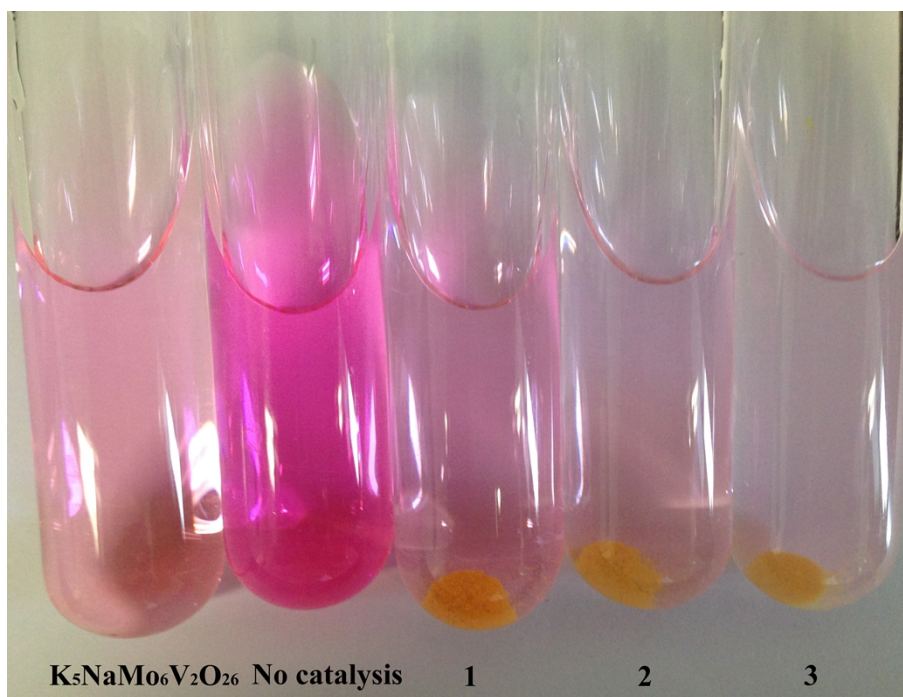


Fig. S11 The color of the RhB solution changes after 9h with catalysts **1**, **2**, **3**, $K_5NaMo_6V_2O_{26}$ and without catalyst.

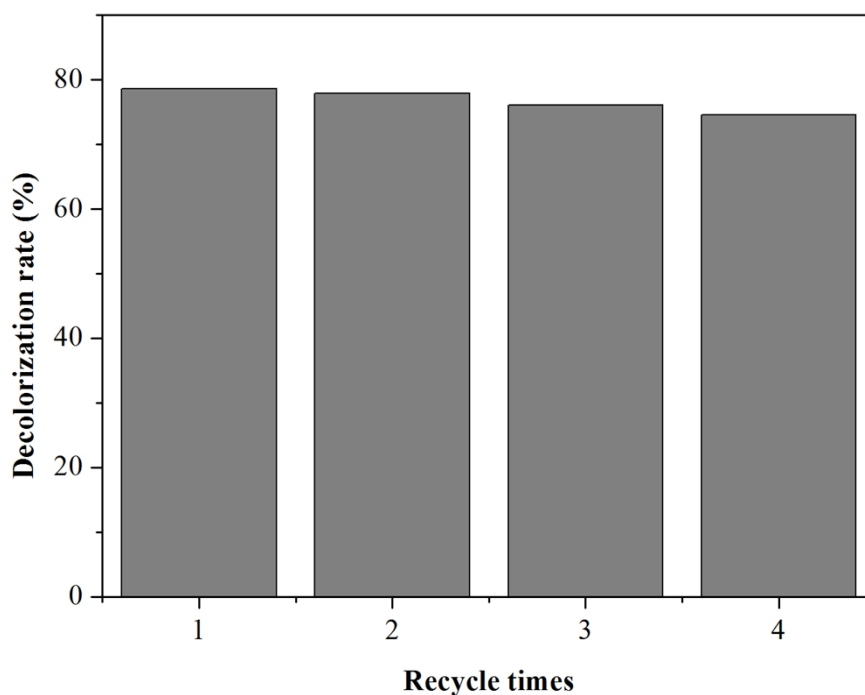


Fig. S12 Effect of number of recycling cycles on the decolorization: photocatalyst **1**, 0.2 g L^{-1} ; RhB, 9.6 mg L^{-1} ; irradiation time, 9h.

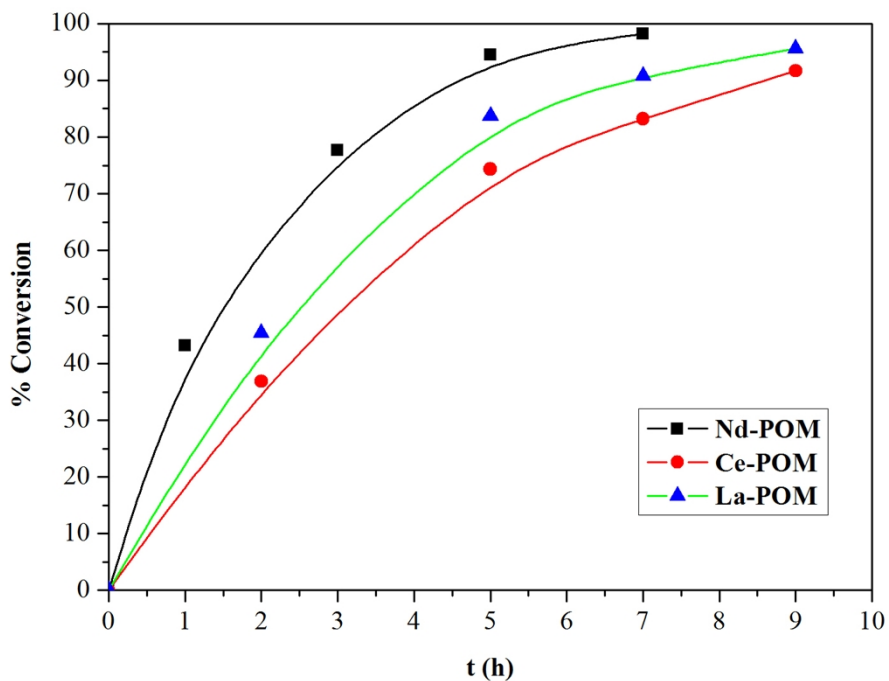


Fig. 13 Kinetic profiles for benzaldehyde cyanosilylation for compounds 1–3.

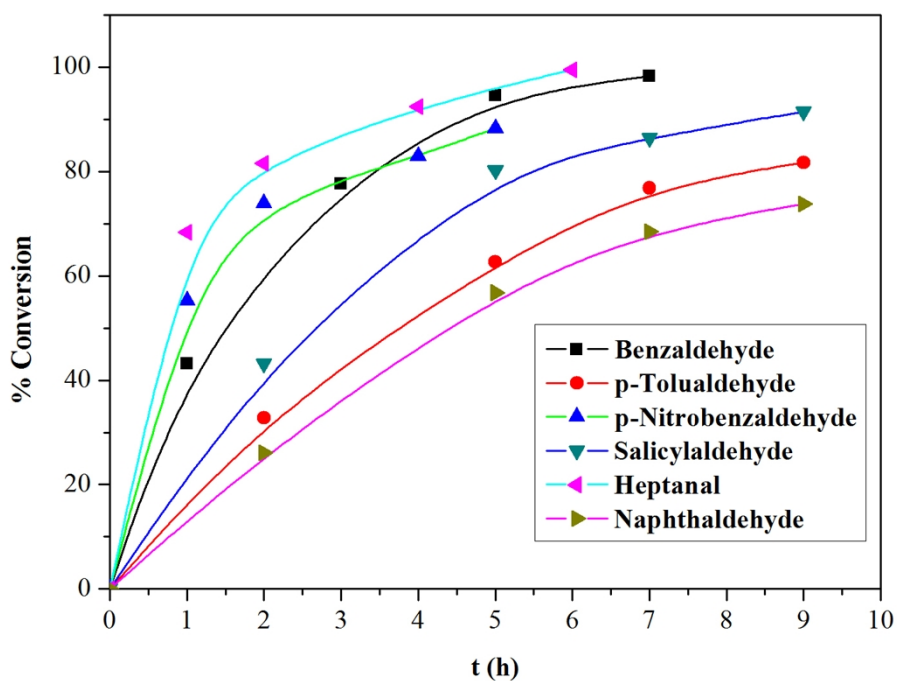


Fig. S14 Kinetic profiles for cyanosilylation for different aldehydes for compound 3.

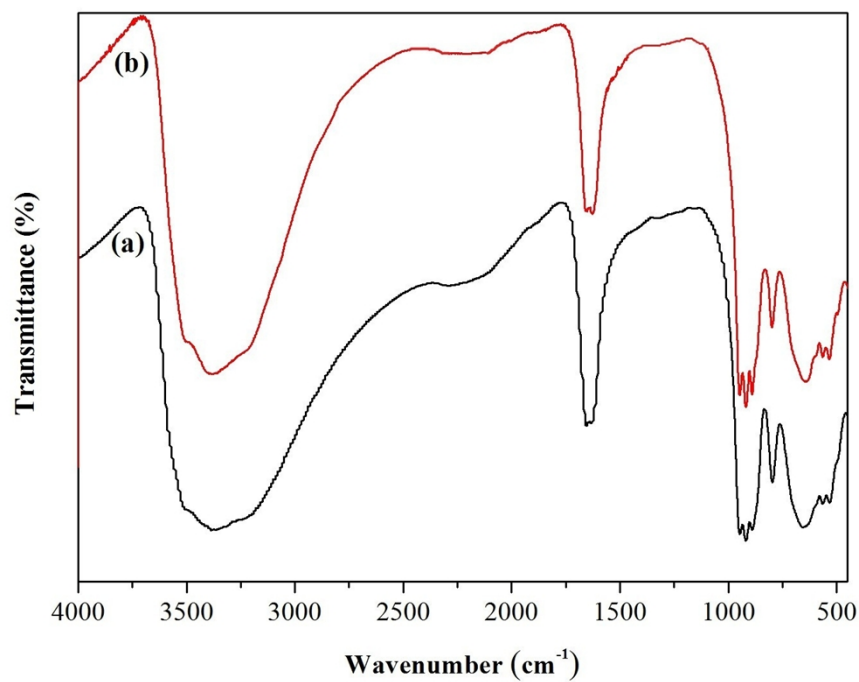


Fig. S15 IR spectrum for (a) as-synthesized compound **3** and (b) recovered catalyst after catalysis reaction.

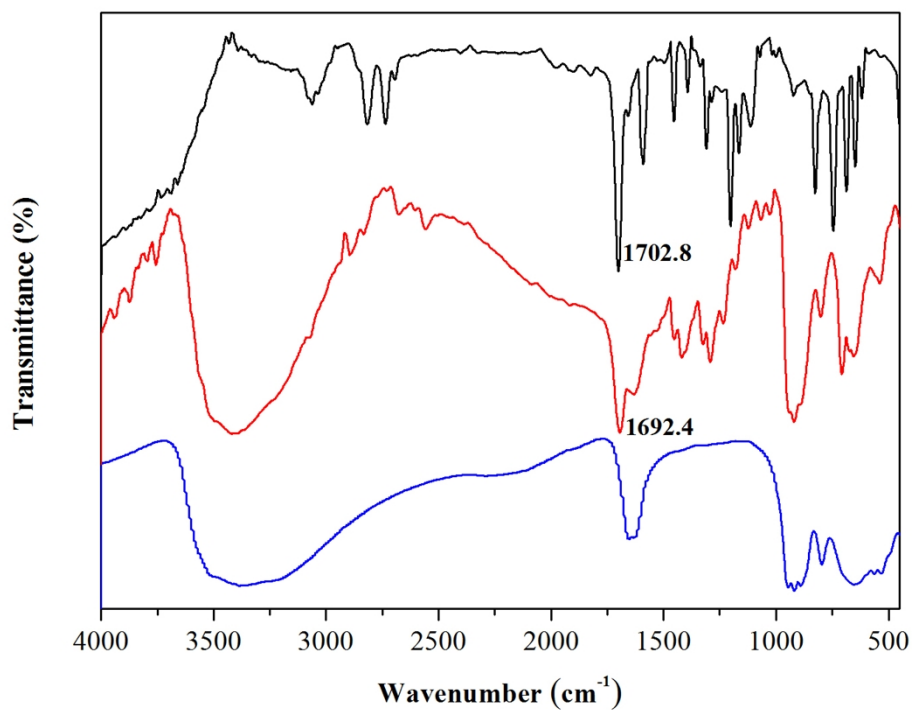


Fig. S16 IR spectra of **3** (bottom) benzaldehyde (top), and **3** obtained after the absorption of benzaldehyde (middle).

IV. Supplementary Tables

Table S1. Study on recycling of catalyst **3** for the heterogeneous cyanosilylation of benzaldehyde in the similar condition.

| Entry | Efficiency(%) |
|---------|---------------|
| Round 1 | 96.2 |
| Round 2 | 95.6 |
| Round 3 | 93.5 |

V. Supplementary Schemes

Scheme S1 Possible mechanism for the cyanosilylation reaction in the case of compound **3**.

